DOI:
10.1016/j.hrthm.2015.04.013

Document Version
Peer reviewed version

An activation-repolarization time metric to predict localized regions of high susceptibility to re-entry

Short title: Act/Repolarization mapping to predict VT site

Authors:

Nicholas Child, BM[1*]; Martin J. Bishop, DPhil[1*]; Ben Hanson, PhD[2]; Ruben Coronel, MD PhD[3,5]; Tobias Opthof, PhD[3]; Bastiaan J. Boukens, PhD[4]; Richard D. Walton, PhD[5,6]; Igor R. Efimov, PhD[4,5,7]; Julian Bostock, PhD[8]; Yolanda Hill, BSc[1], Christopher A Rinaldi, MBBS FHRS[8]; Reza Razavi, MBBS MD[1]; Jaswinder Gill, MD[8]; Peter Taggart, MD DSc[9]

*Joint first authors

Institute:

1. Division of Imaging Sciences, Kings College London, UK.

2. Dept. Mechanical Engineering, University College London, UK.

3. Academic Medical Center, Amsterdam, NL

4. Dept. Biomedical Engineering, George Washington University, USA

5. L'Institut de RYthmologie et de Modelisation Cardiaque (LIRYC), Fondation Université Bordeaux, France

6. INSERM, Universite de Bordeaux, Centre Recherche, Cario-Thoracique de Bordeaux U1045, Bordeaux, France

7. Dept. Biomedical Engineering, Washington University, USA

8. Dept. Cardiology, Guys and St Thomas' Hospital, UK

9. Dept. Cardiovascular Sciences, University College London, UK.

Corresponding author: Dr Nicholas Child, Dept. Imaging Sciences, St Thomas' Hospital, London SE1 7EH, UK.

E-mail: peter.taggart@uclh.nhs.uk Tel:+ 44 2034567898 Fax: +44 20 71885442

Total Word Count: 4972

Grants and Financial Support: The research was supported by the Department of Health via the NIHR comprehensive Biomedical Research Centre award to Guy's & St Thomas' NHS Foundation Trust in partnership with King's College London and King's College Hospital NHS Foundation Trust, and by The Centre of Excellence in Medical Engineering funded by the Wellcome Trust and EPSRC (WT088641/Z/09/Z). MJB is supported by a BHF grant (PG/14/66/30927). BH and PT are supported by an MRC grant (G0901819) and RC is supported by a grant from Marató de TV3. RDW is supported by Agence Nationale de la Recherche (ANR-10-IAHU04-LIRYC).

Industry related disclosures: NC is funded by an Educational Fellowship Grant and JG has an unrelated grant both from St. Jude Medical.

Conflict of Interest: None.

Abstract

Background; Initiation of re-entrant ventricular tachycardia (VT) involves complex interactions between front and tail of the activation wave. Recent experimental work has identified the time interval between S2 repolarization proximal to a line of functional block and S2 activation at the adjacent distal side, as a critical determinant of re-entry.

Objective: We hypothesized that (1) an algorithm could be developed to generate a spatial map of this interval ("re-entry vulnerability index"- RVI); (2) that this would accurately identify a site of re-entry without the need to actually induce the arrhythmia; and, (3) that it would be possible to generate an RVI map in patients during routine clinical procedures.

Methods and Results; An algorithm was developed which calculated RVI between all pairs of electrodes within a given radius. The algorithm successfully identified the region with increased susceptibility to re-entry in an established Langendorff pig heart model and the site of re-entry and rotor formation in an optically mapped sheep ventricular preparation and computational simulations. The feasibility of RVI mapping was evaluated during a clinical procedure by co-registering with cardiac anatomy and physiology of a patient undergoing VT ablation.

Conclusions: We developed an algorithm to calculate a re-entry vulnerability index from intervals between local repolarization and activation. The algorithm accurately identified the region of re-entry in two animal models of functional re-entry. The clinical application was demonstrated in a patient with VT and identified the area of re-entry without the need of inducing the arrhythmia.

Key words:

Arrhythmia

Ventricular Tachycardia

Ablation

Abbreviations

APD – Activation Potential Duration

LV – Left ventricle

RVI – Re-entry Vulnerability Index

VT - Ventricular Tachycardia

Introduction

Ventricular tachycardia (VT) is a well-known precursor of ventricular fibrillation and an important cause of the 300,000 sudden cardiac deaths a year in the USA[1]. The majority of VT episodes are due to re-entry involving a complex interaction between activation and repolarization wavefronts[2-4]. Prerequisites for re-entry are a region of unidirectional block and a region of slowed conduction. The ability to accurately locate ventricular regions of high susceptibility to unidirectional block could have important clinical application.

Unidirectional block is usually functional due to the presence of a region of late repolarization and hence prolonged refractoriness. A premature activation wavefront encountering a region of refractoriness is unable to conduct through the region and is blocked, but travels round the region and approaches the line of block from the distal side. If sufficiently delayed by slowed conduction, such that the proximal region has had time to regain excitability, the returning wavefront may re-excite proximally and form a re-entrant circuit which self perpetuates.

Recent experimental work has demonstrated a mathematical relationship between the relative timing of depolarization and repolarization at upstream and downstream sites located either side of the line of block[5]. In this work, we investigated the hypothesis that an algorithm, which calculates this time interval between every feasible pair of recording sites in a multielectrode map of activation and repolarization times obtained during simple premature stimulation, would successfully identify the site of re-entry upon more aggressive arrhythmia induction. We have designated this time interval the Re-entry Vulnerability Index-RVI.

We consequently developed an algorithm based on a matrix analysis of multiple points and the spatial relationship between subsequent activation and repolarization

intervals between pairs of electrodes during S1-S2 stimulation. We tested the algorithm in two experimental preparations using both multielectrode and optical mapping recordings and confirmed the hypothesis that the RVI map identifies an area which corresponded to the site of re-entry observed with subsequent activation mapping of the arrhythmia. Importantly, the RVI map thus identified *vulnerability* to re-entry even when re-entry did not occur. Such key features were also highlighted with computational simulations, where the region of low RVI was also co-located with the site phase singularity anchoring associated with the re-entry. We subsequently tested the utility of RVI mapping in an in-vivo human ventricle by co-registering with anatomy during a clinical procedure.

Methods

We sought to develop an algorithm that could map the RVI globally, thus identifying spatial regions with high susceptibility to re-entry.

Principles of the RVI algorithm:

Key electrophysiological principles of this algorithm are illustrated in Figure 1 and summarized below:

Following activation (depolarization) myocardial cells are refractory. In a typical re-entry scenario, a premature activation wavefront (S2) encounters a region which has not yet repolarized (Figure 1A), leading to unidirectional block. The wave then travels around the blocked region and re-enters the tissue of origin from the distal side. Whether the wave will be able to return to the starting point and form a re-entry circuit will depend on whether the myocardial cells at the starting point have repolarized. If the wave arrives at the distal side too early it cannot re-excite the

proximal region and will block (bidirectional block, Figure 1B), whereas if it arrives later (Figure 1C) it will successfully re-excite the proximal area. The time interval between the arrival of the wave at the distal region and regaining of excitability (repolarization) in the proximal region is therefore a critical factor[5,6], which we refer to as the RVI.

FIGURE 1

Development of the algorithm for measurement and mapping of RVI

For each recording location RVI is calculated as follows:

First, the S2 beat is identified and the activation and repolarization times from each recording site are measured. For each recording position, neighbouring sites are then identified within a pre-defined radius. Those sites that are activated later than the reference site are identified as "downstream" sites (Figure 2 – *Left*). For each pair of sites, the RVI is then calculated using the algorithm below:

$$RVI_{i,j} = RT_i - AT_j$$

RVI_{ij} = Re-entry Vulnerability Index between electrodes *i* and *j*

RTi = Repolarization time of electrode *i* (proximal)

AT_j = Activation time of electrode *j* (distal) (Figure 2).

This results in a mesh of lines between pairs of points, which in the case of the human example also includes patient-specific ventricular geometry from the clinical mapping system. An RVI map image is then produced from this mesh of lines by associating each RVI value with the geometric mid-point between pairs of points, and plotting the final RVI value as the mean of all values associated with the same location. A color-map is then used in order to highlight small or negative RVI values to reveal the

regions most susceptible to re-entry.

FIGURE 2

Optimization of the algorithm

Prior to its use on animal or human data, the parameters used in the algorithm were optimized using a theoretical analysis of their effect upon the calculated RVI between a pair of electrodes. The search radius of neighboring downstream sites and the spatial resolution of recording electrodes were identified as parameters that could be adjusted to maximize the sensitivity of the algorithm to discriminate between high and low re-entry vulnerability (Supplementary Material (Figure S2) for details).

Validation of the algorithm in an animal model

We tested our algorithm on data from an established animal heart model of repolarization heterogeneity involving a region of shortened APD at the stimulus site and a region of prolonged APD (Figure 4) (details in Supplemental Material and [6]). Activation times and repolarization times for each beat were measured at every mapping electrode site measured using the Wyatt method[7-9] (Figure 3). The RVI mapping algorithm was applied under conditions when re-entry did and did not occur.

FIGURE 3

In the case where re-entry did not occur (Figure 3A), activation spread downwards from the stimulus site (Ω) and blocked as it entered the region of prolonged refractoriness (blue bar). The wavefront then travelled around the region of block (shown as curved white arrows) and arrived at the distal side while the proximal region was still refractory. It was thus unable to establish re-entry (scenario as

depicted in Figure 1B). Figure 3B and 3E shows a similar situation, but in this case the time of arrival of the wavefront at the distal side was later relative to the time of proximal repolarization, and the wave was able to complete a re-entry circuit (scenario as depicted in Figure 1C).

Figures 3C and 3D show the results of RVI mapping corresponding to Figures 3A and 3B respectively. In Figure 3D, the algorithm identified a region where the RVI is very short and re-entry successfully occurred (minimum RVI value -16ms); in Figure 3C, RVI measures were longer and re-entry did not occur (minimum RVI value 29ms). Note, however, that the critical area of susceptibility was still correctly identified even when re-entry did not occur (Figure 3C).

Computational Simulations

Electrical activation was simulated using a monodomain representation of human ventricular tissue over a 2D sheet measuring 10x10cm. Ionic parameters were adjusted to produce a region of prolonged APD in the lower half of the tissue, with shortened APD in the upper half (details in the Supplemental Material). Simulations were performed with the Cardiac Arrhythmia Research Package (http://carp.meduni-graz.at).

Optical Mapping Experiments

Coronary-perfused sheep right ventricular wedges were optically measured using a voltage-sensitive fluorescent dye during induction of re-entry (details in the Supplemental Material).

Application to the human heart

A 63-year old man with a background of ischemic heart disease with recurrent hemodynamically tolerated VT was admitted for a VT ablation. In addition to the standard ablation procedure, a short pacing programme was used for a post-procedure analysis. He had a background of a prior inferior myocardial infarction and had severely impaired systolic function. Antiarrhythmic medications were stopped prior to the procedure. The patient gave informed consent and the local ethics committee approved the study.

The pacing protocol involved pacing from the LV apex using the mapping catheter with an 8 beat S1 drive train with a cycle length of 600ms, followed by an S2 at 500ms. Unipolar electrograms were recorded from a decapolar catheter (Saint Jude Medical, 2mm inter-electrode distance and 5mm spacing between each electrode pair) positioned in the LV (Figure 4). The electrograms and position of electrodes were recorded with Carto3 (Biosense Webster, Ca) with the mapping catheter remaining at the apex as the decapolar catheter was sequentially repositioned to 20 different LV locations to cover the entire endocardial surface (200 recording sites). The same pacing protocol was applied after each repositioning of the decapolar catheter. Low amplitude electrograms with complex morphologies (as typically seen within the perimeter of the scar) were not recorded as these would invalidate the algorithm, with care taken to record normal electrograms just outside these regions (Supplementary Material Figure S3). These measurements did not elicit any VT and the procedure subsequently continued its routine clinical course.

FIGURE 4

Electrophysiological recordings.

Activation and repolarization times were measured using a semi-automated system which first discounts any cases where T-waves are indistinct or corrupt, and then calculates activation and repolarization times with further manual validity check measurements. The algorithm, including error checking, is particularly designed for robust measures in the presence of noise; and has previously been described in detail[10].

Results

Computational Simulations

Figure 5 shows an example of a premature (Case (ii), re-entry initiated) and slightly less premature (Case (i), bidirectional block) S2 beat simulated within a heterogeneous 2D sheet. The respective voltage map images (panels 5A & 5D) and activation maps (panels 5B, 5E, 5F) show similar wavefront and wavetail dynamics compared to the experimental preparation (Figure 3). In both Cases (i) and (ii), the S2 wavefront is initially blocked as it encounters refractory tissue in the region of long APD, travelling around the line of block and eventually entering the distal region of prolonged APD as it recovers. In Case (ii), the wavefront is able to propagate into recovered tissue at the site of initial block to successfully re-enter (panel 5F), whereas the tissue remains refractory in Case (i) and bidirectional block occurs. Panel 5G shows the computed RVI map for Case (ii), highlighting that the region of low RVI is distinctly co-located with the site of initial block and re-entry. Importantly, as in Figure 3, the corresponding RVI map for the case of failed re-entry (Case (i)) also shows low RVI values in a similar site (panel 5C). Finally, for the case of sustained

re-entry (Case (ii)), a 'hot-spot' map of cumulative phase singularity locations is shown (panel 5H), highlighting that the region of spiral wave rotor clustering occurs adjacent to the region of low RVI. Movies of all simulations can be found in Supplemental Material.

FIGURE 5

Optical Mapping

Figure 6 shows sequential fluorescent images (panel 6A) and corresponding activation maps (panel 6B, 6C) for the premature S2 beat during a case of induced re-entry in the experimental coronary-perfused sheep right ventricular preparation, described above. The S2 wavefront is initially blocked (110ms image), but eventually propagates around this region of block and re-enters (220ms). Panel 6D shows example optical APs from two pixels located proximal (blue triangle) and distal (green star) to the line of block. Finally, panel 6E shows the computed RVI map; as expected the region of low RVI is co-located with the site of initial block and re-entry.

FIGURE 6

RVI map to predict location of exit point in a patient undergoing VT ablation

In order to test the feasibility of RVI mapping during clinical procedures, the algorithm was applied to the activation/ repolarization mapping data obtained at 200 LV endocardial sites in a patient with a previous myocardial infarction undergoing a routine VT ablation procedure.

Figure 7 shows the spatial distribution of the RVI calculated based-on the S1-S2 protocol that did not result in the induction of an arrhythmia. The shortest values, which represent sites of highest susceptibility to re-entry (dark red), are confluent in the postero-basal region.

FIGURE 7

Subsequently, a spontaneous hemodynamically tolerated VT was induced following an isoprenaline bolus, with the same cycle length (CL 430ms) as the clinical VT. The VT circuit was identified during the arrhythmia through a combination of activation mapping (Supplementary Material Figure S4) and locating diastolic potentials (Supplementary Material Figure S5). It was also demonstrated that entrainment occurred with concealed fusion with a post-pacing interval only slightly longer than the VT cycle length (Supplementary Material Figure S6). Radiofrequency ablation was performed in this region (Supplementary Material Figure S7) terminating the VT, which was then no longer inducible and there has been no further VT episodes since. Superimposition of the RVI with scar, and circuit exit point is shown in Figure 8

FIGURE 8

Discussion

We have developed a mapping algorithm able to identify localized regions of high susceptibility to conduction block and re-entry using a novel parameter referred to as the re-entry vulnerability index (RVI) based on our previous experimental work[5]. In an animal model of repolarization heterogeneity (mimicking the peri-infarct region) in which re-entry had been induced and mapped, the algorithm successfully identified the region of block and subsequent re-entry. It also performed similarly well in optical

mapping experiments and computer simulations in which it also co-located regions of low RVI with spiral wave rotors. We then applied this technique to a patient undergoing radiofrequency VT ablation in whom activation and repolarization times were measured from 200 electrode sites in the LV during S1-S2 pacing that did not induce the arrhythmia. From these data points the algorithm generated a global map of RVI that could be co-registered with the anatomy. It is of note that the low RVI co-located with the VT exit site identified after induction of the arrhythmia.

Optimization and experimental validation of the RVI mapping algorithm

Theoretical sensitivity analysis of the dependence of the RVI metric magnitude with respect to parameters used in its calculation allowed us to optimize the algorithm to robustly distinguish regions of block/re-entry when applied to different experimental, modelling and clinical applications, and across different species (sheep, porcine, man). In porcine experiments and computer simulations, re-entry was established due to an imposed intrinsic gradient of repolarization, whereas in the sheep optical mapping experiments, re-entry was established following a strong cross-field shock perpendicular to a uniform repolarization wave, setting-up initial conduction block. In all cases, however, the algorithm successfully identified the site of re-entry.

Our approach links the classical views on re-entry posited by Mines, to those involving the more mathematical description of rotors, wavefront-wavetail interaction, and singularity points. The RVI is based on the interaction between the front and the tail of an activation wave across a region of block (Figure 1), being functional (Figures 3, 5 & 6) or structural (Figures 7-8) in nature. We demonstrate that without addressing the underlying mechanism of re-entry (either leading circle[2]

or rotor based [2,3]) the algorithm accurately identifies the site of re-entry. This is of clinical importance, because this is the site that is the target for ablation therapy.

Our RVI metric is based upon electrophysiological parameters that have a long established importance in arrhythmogenesis, activation time, repolarization time. The main significance of our index is that it allows identification of the site of initiation of re-entry without the need to actually induce the arrhythmia (which is usually clinically hemodynamically not tolerated or inducible); in contrast, identifying phase singularities requires a rotor to be induced. In our simulations, we were also able to demonstrate a strong, but not exact, correlation of the region of low RVI with the site around which phase singularities associated with the rotor clustered. These regions could also be approximately identified from activation time maps where CV slowed near the rotor core. However, in addition to the fact that CV may be undefined at the site of block, the area identified as low RVI corresponded to a much smaller region than the area of slowed CV, spanning only the line of block at the localised area where re-entry occurs for the first time. We further note that our RVI approach will identify sites vulnerable to re-entry in situations in which singularity points are not always present, for example during anatomical re-entry, thus working equally well regardless of the underlying re-entry mechanism.

A low RVI is pro-arrhythmic and is enhanced by shorter APD of the premature S2 in the proximal zone (see Figure 1C). Repolarization in the proximal region is determined by the local APD restitution characteristics. Steep APD restitution in this region therefore would be potentially pro-arrhythmic (shorter RVI) and conversely flattening restitution would be potentially anti-arrhythmic (longer RVI). This would

be in keeping with the classic restitution hypothesis[11] and the known anti-fibrillatory effect of flattening APD restitution[12], although the latter considerations are likely more relevant to non steady-state conditions. Our data also demonstrate that a slope of the restitution curve needs not to be higher than 1 to identify pro-arrhythmic conditions.

Clinical Application

RVI mapping is clinically applicable in the treatment of VT by radiofrequency ablation, where success rates overall are unsatisfactory[13]. The majority of VT episodes following myocardial infarction are due to re-entry mechanisms, involving interaction between electrical activation and repolarization waves[4].

Clinical ablation procedures typically focus on activation times rather than measure repolarization times in order to localize the circuit, and when this is not possible anatomic mapping is usually performed (identifying areas with low amplitude signals, that may not be involved in a re-entrant circuit). Whereas an activation map might be expected to identify a region of block, it would not indicate whether re-entry could occur back through the region of block without the induction of the arrhythmia. We constructed an activation map (Supplementary Material Figure S8) which shows crowding of isochrones indicating slowed activation at the site of minimum RVI in Figure 7. Although this finding supports the existence of block at this site, it does not provide any indication as whether re-entry may occur, similar to the cases shown in Figures 4A and 5A. Activation mapping of the induced arrhythmia confirmed that the site of lowest RVI corresponds to the site of re-entry.

Clinically, the optimum ablation strategy aims to prevent the arrhythmia by interrupting the re-entry pathway by delivering RF energy to the isthmus and around the scar[14,15]. However, this is only possible in a minority of cases, either because the arrhythmia is not hemodynamically tolerated or the VT is non-inducible. Furthermore, multiple exits may exist that may remain undetected by these standard methods[14].

In ischemic cardiomyopathy, re-entrant arrhythmias are based on anatomic re-entry involving the scar region, which provides the electrophysiological requirements of heterogeneous activation and repolarization for initiating and maintaining the re-entry circuit. The re-entrant activation commonly involves conduction along channels of surviving myocardium that transect the infarcted region. Although conduction velocity along these surviving fibers is typically normal[16,17], the tortuosity of the channels causes a relatively long pathway and thereby a long conduction delay. If the surviving fibers connect to non-infarcted myocardium, circular activation can be accomplished. The apparent 'focal' origin of the tachycardia in reality is the exit point where the re-entrant activation emanates from the infarcted tissue. Experiment and theory predict that the site of unidirectional block in post infarct VT is located near the exit point[18]. Additional conduction delay is often provoked by a premature beat[19] and the completion of full re-entry depends on whether the normal tissue has regained excitability following the premature beat. These are the conditions identified by the RVI algorithm. The algorithm has the potential advantage that it does not require initiation of the tachycardia and employs non-critical prematurity of extra stimulation.

Limitations

We cannot exclude the possibility that some variations in the post MI substrate such as post repolarization refractoriness might affect the clinical performance of the algorithm. Post repolarization refractoriness, if present, is likely to occur in the region of block; in which case, the normal correspondence between action potential repolarization and refractoriness may not exist. However, our algorithm does not incorporate the time of action potential repolarization in the downstream region of block, only the activation time in this region of the premature beat, together with the repolarization time of the premature beat in the upstream region. Therefore, post repolarization refractoriness does not affect the efficacy of the RVI algorithm.

The study in one patient was intended to verify the prediction that an RVI map could be generated in the human ventricle during the course of a clinical procedure and that the RVI map could be co-registered with geometry acquired using a Carto mapping system (Biosense Webster, Ca). No attempt is made at this stage to establish a role for RVI mapping as an aid to ablation other than to demonstrate its feasibility. Future work may identify the efficacy, sensitivity and specificity of this combined activation and repolarization mapping approach in radiofrequency ablation procedures in larger cohorts of patient with VT.

References

1. Lopshire JC, Zipes DP. Sudden cardiac death: better understanding of risks, mechanisms, and treatment. *Circulation* 2006;114:1134-6.

2. Comtois P, Kneller J, Natter S. Of circles and spirals: bridging the gap between the leading circle and spiral wave concepts of cardiac re-entry. Europace 2005: 7: 10-20.

3. Panfilov AV. Theory of re-entry. In: Cardiac Electrophysiology: From Cell to Bedside. 4th edition. Eds. Zipes DP, Jalife J. Publ. Saunders, Chpt 31, 2009.

remove 2,3,4,6,7

4. Gough WB, Mehra R, Restivo M, Zeiler RH, El-Sherif N. Re-entrant ventricular arrhythmias in the late myocardial infarction period in the dog. 13. Correlation of activation and refractory maps. *Circ Res* 1985;57:432-42.

5. Coronel R, Wilms-Schopman FJ, Opthof T, Janse MJ. Dispersion of repolarization and arrhythmogenesis. *Heart Rhythm* 2009;6:537-43.

6. Coronel R, Wilms-Schopman FJ, Janse MJ. Anti- or profibrillatory effects of Na(+) channel blockade depend on the site of application relative to gradients in repolarization. *Front Physiol* 2010;1:10.

7. Wyatt RF BM, Evans AK. Estimation of ventricular transmembrane action potential durations and repolarization times from unipolar electrograms. *Am J Cardiol* 1981;47:488.

8. Coronel R, de Bakker JM, Wilms-Schopman FJ, Opthof T, Linnenbank AC, Belterman CN, Janse MJ. Monophasic action potentials and activation recovery intervals as measures of ventricular action potential duration: experimental evidence to resolve some controversies. *Heart Rhythm* 2006;3:1043-50.

9. Haws CW, Lux RL. Correlation between in vivo transmembrane action potential durations and activation-recovery intervals from electrograms. Effects of interventions that alter repolarization time. *Circulation* 1990;81:281-8.

10. Western D, Taggart P, Hanson B. Real-time feedback of dynamic cardiac repolarization properties. *IEEE Eng Med Biol Soc Conf* ;2010:114-7.

11. Riccio ML, Koller ML, Gilmour RF, Jr. Electrical restitution and spatiotemporal organization during ventricular fibrillation. *Circ Res* 1999;84:955-63.

12. Garfinkel A, Kim YH, Voroshilovsky O, Qu Z, Kil JR, Lee MH, Karagueuzian HS, Weiss JN, Chen PS. Preventing ventricular fibrillation by flattening cardiac restitution. *PNAS* 2000;97:6061-6.

13. Aliot EM, Stevenson WG, Almendral-Garrote JM, Bogun F, et al. EHRA/HRS Expert Consensus on Catheter Ablation of Ventricular Arrhythmias. *Heart Rhythm* 2009;6:886-933.

14. Stevenson WG, Delacretaz E. Radiofrequency catheter ablation of ventricular tachycardia. *Heart* 2000;84:553-9.

15. Ponti RD. Role of catheter ablation of ventricular tachycardia associated with structural heart disease. *World J Cardiol* 2011;3:339-50.

16. de Bakker JM, Coronel R, Tasseron S,et al. Ventricular tachycardia in the infarcted, Langendorff-perfused human heart: role of the arrangement of surviving cardiac fibers. *J Am Coll Cardiol* 1990;15:1594-607.

17. de Bakker JM, van Capelle FJ, Janse MJ, Tasseron S, Vermeulen JT, de Jonge N, Lahpor JR. Slow conduction in the infarcted human heart. 'Zigzag' course of activation. *Circulation* 1993;88:915-26.

18. Segal OR, Chow AW, Peters NS, Davies DW. Mechanisms that initiate ventricular tachycardia in the infarcted human heart. *Heart Rhythm* 2010;7:57-64.

19. Saumarez RC, Camm AJ, Panagos A, Gill JS, Stewart JT, de Belder MA, Simpson IA, McKenna WJ. Ventricular fibrillation in hypertrophic cardiomyopathy is associated with increased fractionation of paced right ventricular electrograms. *Circulation* 1992;86:467-74.

Legends for figures

Figure 1 – Illustration of RVI in cases of re-entry and block. APDs are shown for the last 2 beats of a steady state train (S1) followed by a premature beat (S2). Activation conducts from proximal sites (upper rows) to distal sites (lower rows) as indicated by arrows. The interval between the time of arrival of the premature S2 beat at the distal site and repolarization of the premature S2 beat proximally (represented in panel B and C by varying thickness of the vertical grey bars) is a critical determinant of whether re-entry will occur and is referred to as the Re-entry Vulnerability Index (RVI). Adapted from Coronel et al.[6].

Figure 2. RVI mapping *Left* - Activation wave (red) shown propagating through region of a recording electrode grid (black circles), with the current proximal recording electrode shown in pink. All downstream distal electrodes within a set radius are shown in blue. *Right* - RVI_{ij} is calculated as the difference between the repolarization time of the *i*th proximal electrode (RT_i) and the activation time of each *j*th distal electrode (AT_j) on the S2 beat.

Figure 3. Animal experiments. Activation sequence after premature stimulation (S2) from an experiment in a Langendorff pig heart model of inhomogeneous repolarization (APD shortened by Pinacidil above the dashed line and prolonged by sotalol below the dashed line) in the cases of unsuccessful (A) and successful (B) re-entry. The premature wavefront propagates from the stimulation site (Ω) and is recorded by the electrode grid (electrodes represented by dots). C & D show

corresponding RVI maps, with the critical area of low RVI identified in D. E shows activation sequence of the first re-entrant beat.

Figure 4. Data Collection. A - Recordings of LV endocardial unipolar electrograms recorded via the Ensite 3000 system during steady state (S1) and premature activation (S2). B – Position of catheters on fluoroscopy (A – ablation catheter, D – decapole catheter, R – RV Apex catheter, ICD – ICD lead). C – Local activation and recovery times of the unipolar electrogram (following S2) were measured by the Wyatt method[7].

Figure 5. Computational simulations. Simulations of premature S2 beats in the cases of bidirectional block (S2 interval 350ms, upper panels) and unidirectional block and re-entry (S2 interval 340ms, lower panels). In each case voltage maps showing activation sequences (A, D), activation maps (B, E, F) and calculated RVI maps (C, G) are shown. Phase singularities are shown as pink circles in panel D. In the case of re-entry, a 'hot-spot' map showing cumulative spatial phase singularity locations is shown (panel H). All timings shown are relative to S2 application.

Figure 6. Optical mapping. Normalized fluorescent voltage maps showing activation sequence (panel A), activation maps (panel B, & C) and calculated RVI map (panel E) following a premature S2 beat that successfully initiated re-entry. Panel D shows example fluorescent traces from a region proximal (blue) and distal (green) to the line of block. All timings shown are relative to S2 application.

Figure 7. Clinical RVI Map. A – Diagrammatic representation of the LV showing a map of the spatial distribution of the RVI. B – RVI mapped on the 3D Carto geometry, displayed in the left lateral and right anterior oblique projections.

Figure 8. Correlation of RVI with VT. *Left* – Diagrammatic representation showing superimposed scar (white), activation sequence (white arrow) and area of low RVI (dark red area) co-localizing with VT exit point (yellow). *Right* – Carto geometry with the same features displayed on the left lateral projection of the 3D geometry. Small red dots show areas of endocardial ablation which resulted in termination and non-inducibility of the VT. White arrow represents the direction of circuit on leaving the exit point deduced from the activation map (Supplemental Material Figure S8).

Figures

Figure 1

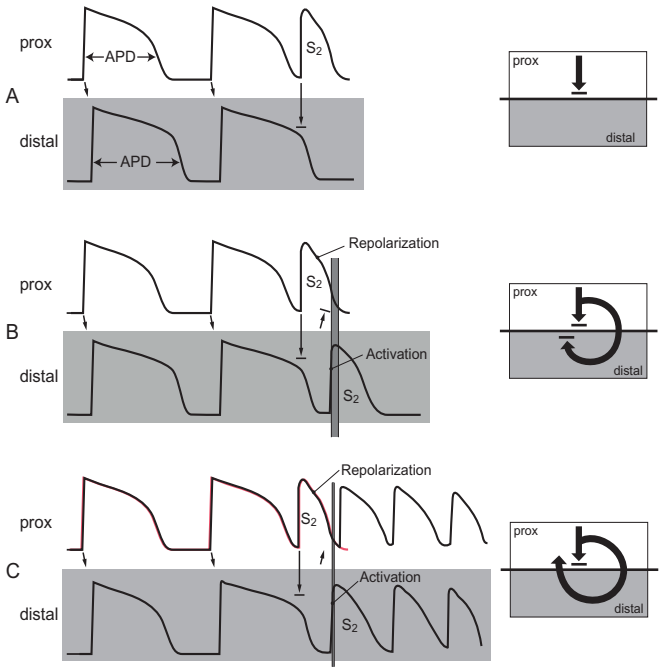

Figure 2

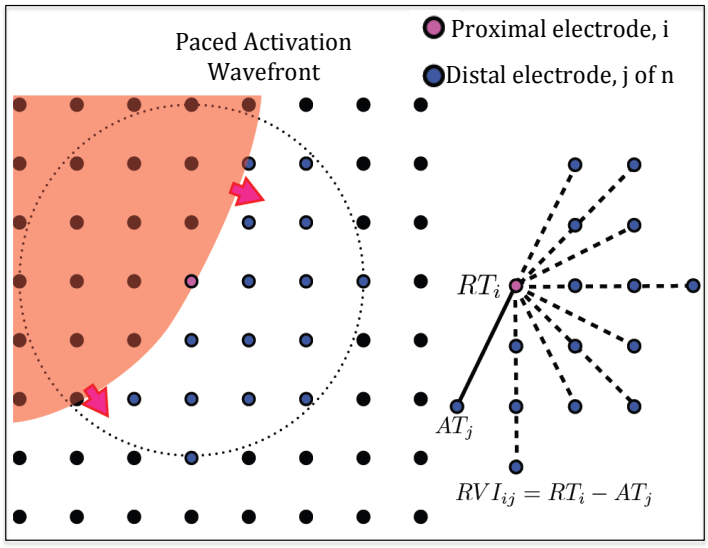

Figure 3

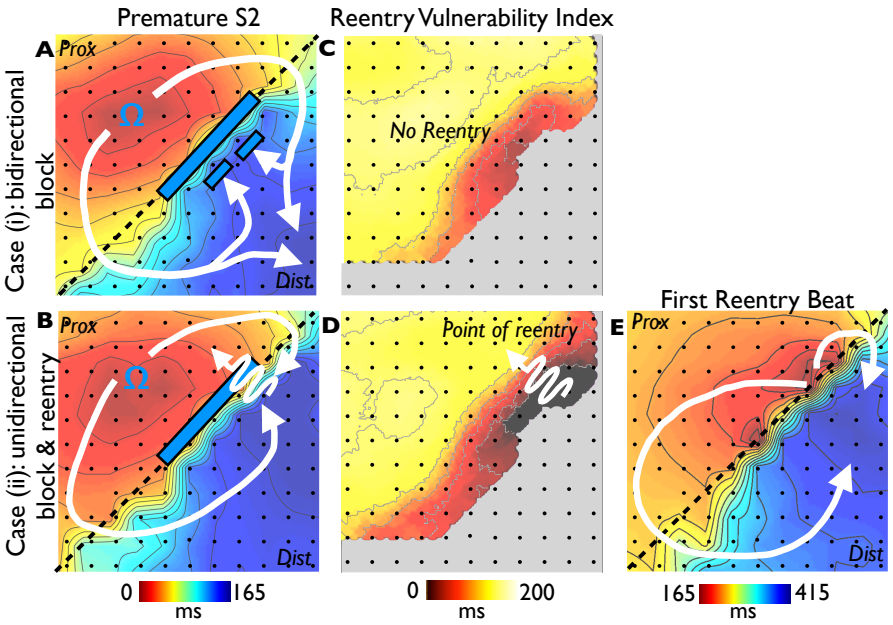

Figure 4

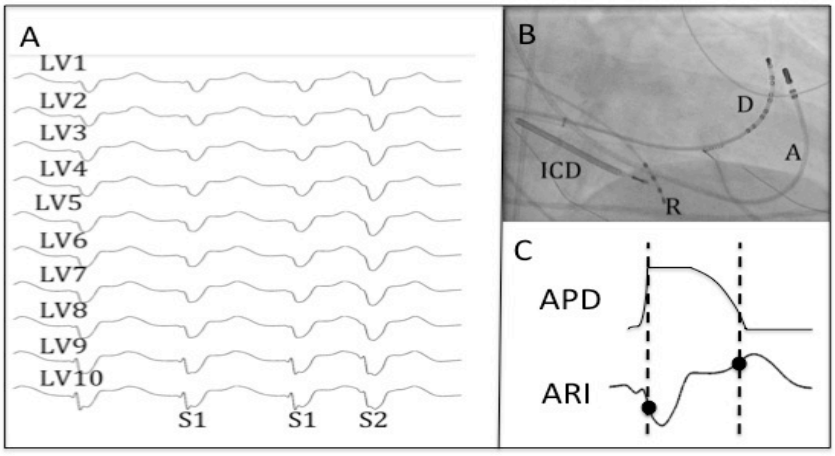

Martin Bishop 18/3/15 15:56
Comment [1]: Change limits

Figure 5

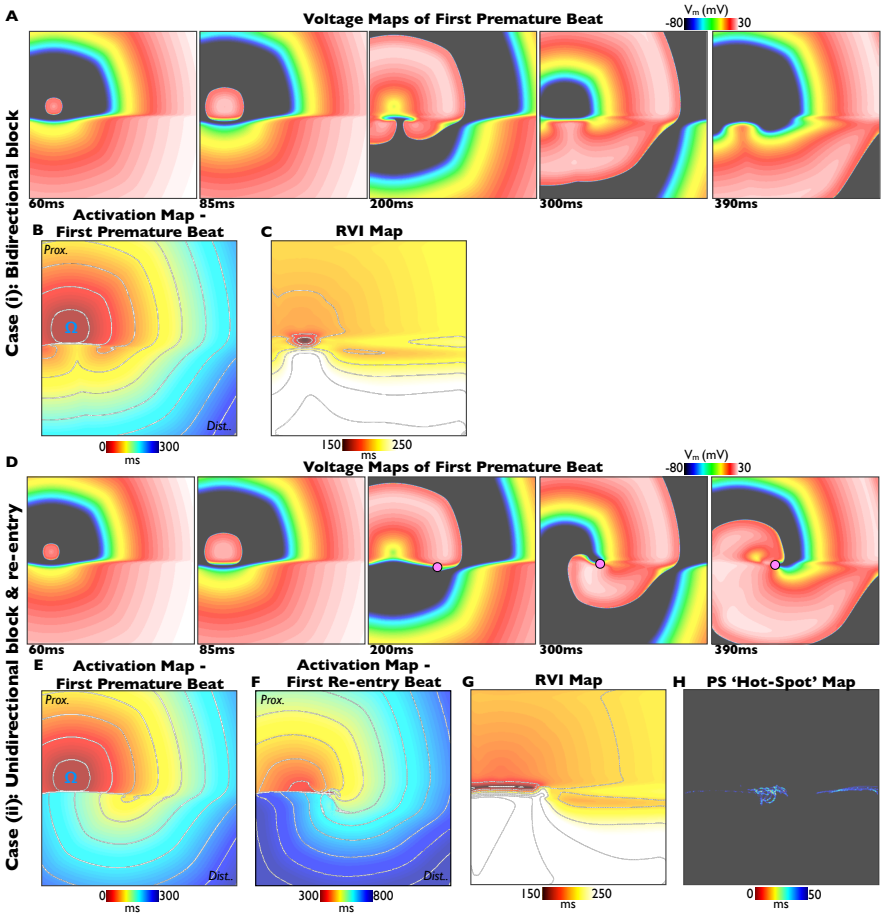
A
Voltage Maps of First Premature Beat
Vm (mV)
-80
30
Case (i): Bidirectional block
60ms
85ms
200ms
300ms
390ms
B
Activation Map - First Premature Beat
C
RVI Map
Prox.
Dist.
0
300
ms
150
250
ms
D
Voltage Maps of First Premature Beat
Vm (mV)
-80
30
Case (ii): Unidirectional block & re-entry
60ms
85ms
200ms
300ms
390ms
E
Activation Map - First Premature Beat
F
Activation Map - First Re-entry Beat
G
RVI Map
H
PS 'Hot-Spot' Map
Prox.
Dist.
0
300
ms
300
800
ms
150
250
ms
0
50
ms

Figure 6

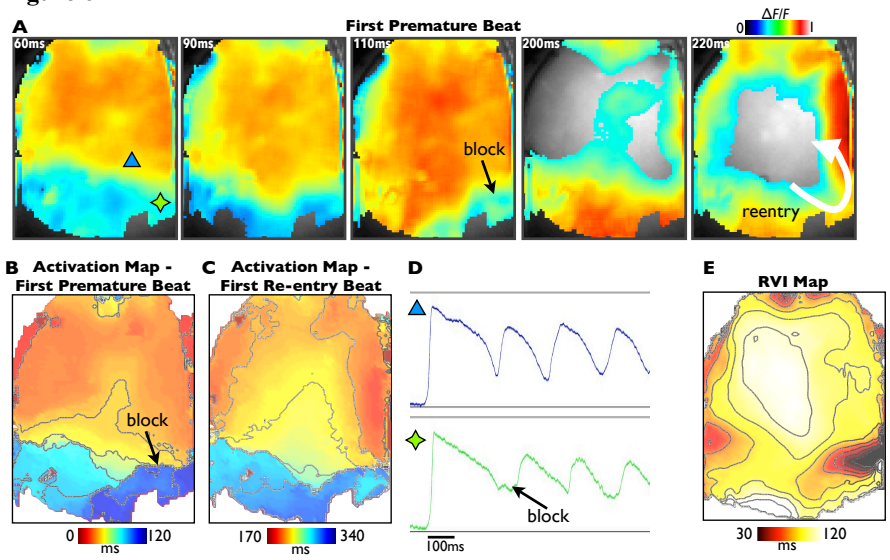

Figure 7

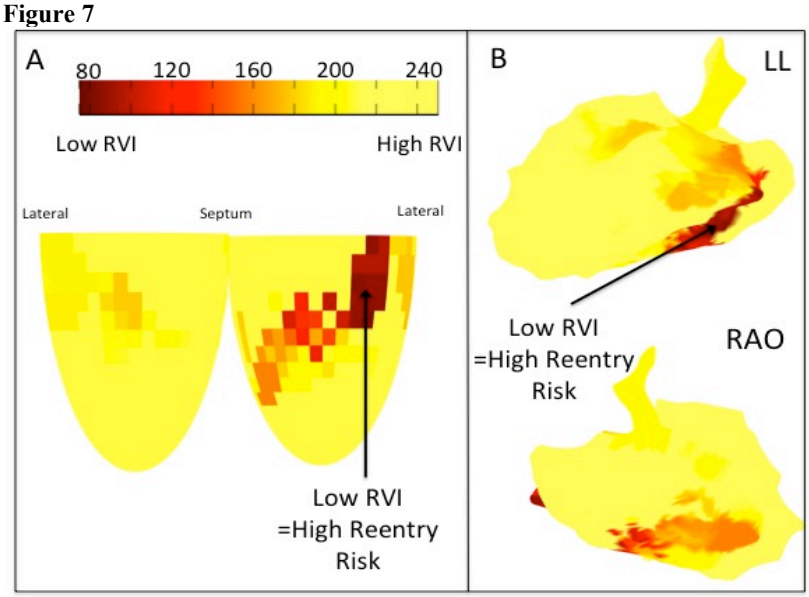

Figure 8

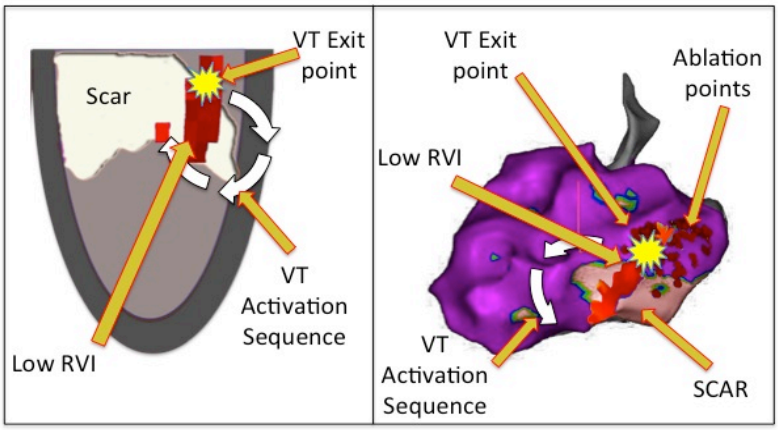
VT Exit point
Scar
VT Activation Sequence
Low RVI
VT Exit point
Ablation points
Low RVI
VT Activation Sequence
SCAR